JOURNAL OF MATERIALS SCIENCE 30 (1995) 4637–4644

Effect of carbon sources on the combustion synthesis of TiC

YOON CHOI, SHI-WOO RHEE
Laboratory for Advanced Materials Processing, Department of Chemical Engineering, Pohang University of Science and Technology, Pohang 790-784, Korea

The effect of carbon sources, i.e. graphite and amorphous carbon, on the reaction mechanism, product morphology, and the rate of combustion reaction between Ti and C to form TiC were studied. A reaction mechanism was proposed for each carbon source from the activation energy of combustion reaction. The microstructure and the composition of reaction products were also investigated. It was observed that graphite fissured in a layered form during the combustion reaction and the reaction between graphite and liquid titanium was accomplished mainly on the surface of the thinly fissured layer. Graphite was found to be more reactive with titanium and titanium carbide synthesized with graphite contains less amount of unreacted carbon and is more close to the stoichiometric TiC.

1. Introduction

In the combustion synthesis of ceramic materials, the reaction is highly exothermic and the heat liberated can sustain the reaction with a combustion wave propagating until the reactants are converted into the product. This process is also known as self-propagating high-temperature synthesis (SHS). In the last two decades, this method has been successfully applied to the synthesis of various materials including carbides [1,2], borides [3,4], nitrides [5,6], intermetallics [7–9], and composite materials [10,11]. Recently it has also been applied to make ceramic-lined metallic pipes [12]. The combustion wave structure [13,14] has also been studied to explain the heat and mass transfer in a chemically reacting system.

Combustion synthesis of titanium carbide from titanium and carbon powders has been studied with considerable interest as an alternative to conventional processes [15,16] such as carbothermal reduction of TiO_2, because it is simple and energy-efficient. TiC has good hardness, high-temperature stability, high electrical conductivity, and chemical resistance [16]. TiC has a metallic appearance, and its electrical and thermal conductivity are comparable to stainless steel [17]. Titanium carbide, like the other group IV transition metal monocarbides, exists over a very wide range of carbon–titanium ratio, $TiC_{0.97}$ to $TiC_{0.47}$ [17].

The reaction between titanium and carbon has been studied by various methods. Vadchenko and coworkers [18] investigated the ignition and combustion process between titanium and carbon by using carbon-coated titanium wires. With transmission electron microscopy, Korchagin and Aleksandrov [19] studied the interaction between thin layers of titanium and carbon. A review of reactant transport at the Ti–C interface by molecular dynamics simulation was made [20]. The reaction between titanium and carbon powders has also been studied by gradually changing the stability of the combustion front. It has been performed by igniting reactant mixtures placed in a wedge-shaped cavity in a copper block [21]. Recently Wong and colleagues [22] monitored phase transformation during the combustion reaction between titanium and amorphous carbon by real-time diffraction using synchrotron radiation. They reported that TiC formation was completed within 400 ms after the melting of Ti metal, indicating that TiC formation took place during the passage of the combustion wave front. The effect of aluminium [23], iron and cobalt [24] addition on the combustion reaction of Ti and C has been studied by Choi and Rhee. They also studied the equilibrium in the reaction of Ti and C to form substoichiometric TiC_{1-x} [25].

The elementary reaction in titanium carbide synthesis is as follows [26]

$$Ti + C \rightarrow TiC, \quad \Delta H^0_{f,298} = -184.502\ kJ\,mol^{-1}.$$

This heat of reaction is large enough to sustain a combustion wave propagation, once the reaction is initiated. Khaikin and Merzhanov [27] formulated and calculated the propagation velocity by assuming that the reaction is homogeneous, and it mainly proceeds in a narrow reaction zone close to the maximum temperature, and the convective and radiative heat losses can be neglected. They derived the expression for the combustion wave velocity in exothermic reaction. The apparent activation energy for the combustion reaction can be determined from an Arrhenius plot of $\ln[(1-w)^{1/2}u/T_c]$ versus $1/T_c$, once the combustion temperature (T_c) and wave velocity (u) have been measured [28,29]. Here, w is the weight fraction of the diluent.

0022–2461

TABLE I Description of precursor powders

Designation	Description	Manufacturer	Purity (wt %)	Particle size (μm)	Surface area ($m^2 g^{-1}$)
Ti	Titanium	Kojundo Kagaku Co.	99.9	30	0.56
C1	Graphite	Kojundo Kagaku Co.	99.9	5	19.8
C2	Graphite	Cerac, Inc.	99.9	15.2	7.69
C3	Furnace black (Vulcan XC-72R)	Cabot	99.0	0.030	254
C4	Furnace black (Black Pearls 120)	Cabot	99.5	0.075	25
TiC	Titanium carbide	Kojundo Kagaki Co.	99.9	3.5	2.68

Amorphous carbon has been extensively used as a carbon source in the combustion synthesis of TiC. Amorphous carbon may be considered as sections of hexagonal carbon layers of varying size, with very little order parallel to the layers [30]. On the other hand, graphite is characterized by a well-developed layer structure in which the atoms are arranged in open hexagons and the layers have some order in stacking sequence [30]. In the reaction mechanism study by wave velocity method using combustion parameters, the previous researchers of Kirdyashkin and co-workers [31] and Dunmead and colleagues [32] used lamp black and furnace black, respectively.

In this work, crystalline graphite and amorphous furnace black powders were used and the effects of each carbon source on TiC combustion synthesis were studied. In fact, little information exists related to the effect of the structure of carbon on the reaction mechanism and reactivity in TiC combustion synthesis. Rate measurements in the combustion synthesis of TiC using carbon sources with different crystallinity will give us some insight as to the reaction mechanism between carbon and titanium.

We investigated the reaction products which were formed by combustion reaction and reaction couple methods. Optical and scanning electron microscopy (OM, SEM), X-ray diffraction (XRD), and wet chemical methods were used to study the morphology, crystallographic relationship, and composition of synthesized titanium carbide.

2. Experimental methods

Table I shows the characteristics of titanium, graphite, furnace black, and titanium carbide powders used as starting materials. The reactant mixture with the desired composition was mixed in a dry mixer for about 15 h. Cylindrical compacts 20 mm in diameter and approximately 30 mm in height were formed at pressures from 70 to 76 MPa in a stainless steel die with double-acting rams. The green density of the compact was maintained at 62 ± 3% of theoretical.

Fig. 1 shows the schematic diagram of the set-up. As shown in Fig. 1, a hole about 2 mm in diameter and about 10 mm in depth was formed in the side of the pellet to serve as a black-body hole. The temperature was measured by focusing the optical pyrometer (TR-630A, Minolta Camera Co.) equipped with a close-up lens on the black-body hole of the sample.

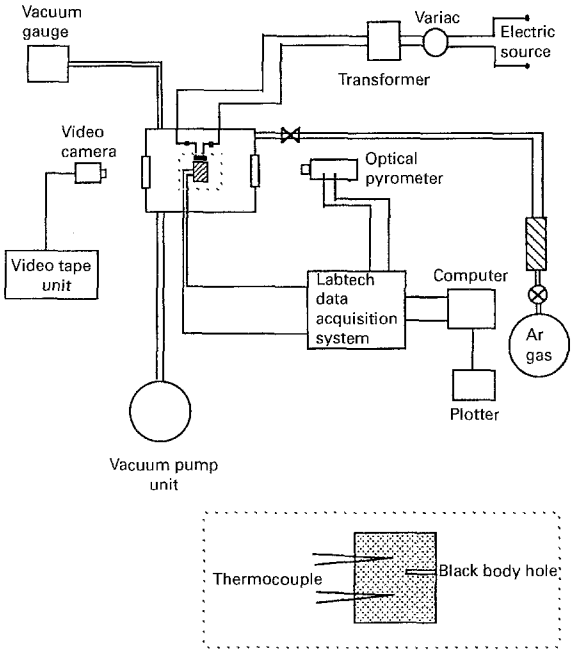

Figure 1 Schematic diagram of the experimental apparatus for combustion synthesis.

The i.r. absorption was calibrated by using a black-body furnace (UIK-T009A, Chino Co.). Two small W–Re thermocouple wells of size 0.254 mm were inserted in the opposite side of the wall with a gap of 15 mm. Pellets were dried in a vacuum dry oven for 24 h at 573 K and 10^{-4} Torr. The dried pellet was placed in a stainless steel chamber with two quartz windows. The chamber was 270 mm high with a diameter of 160 mm. A zigzag shaped tungsten filament was positioned approximately 2 mm above the top surface of the pellet for ignition. The chamber was purged and filled with argon gas before the ignition. The top surface of the sample was ignited by applying current of about 80 A to the filament under about 50 V from a 7 kW transformer. The ignition occurred almost instantaneously with the application of current for all the samples, regardless of carbon sources.

The real time voltage outputs from the W–Re thermocouple and the optical pyrometer were continuously recorded using a data acquisition system and personal computer. The propagation of the combustion wave was recorded by a video camera capable of replaying the reaction by 1/30 s. To minimize the end effect at the top and bottom of the sample, the com-

TABLE II Experimental parameters of TiC combustion synthesis

Composition (mole ratio, wt %)		T_c (K)	u ($cm\,s^{-1}$)	Composition (mole ratio, wt %)		T_c (K)	u ($cm\,s^{-1}$)
Ti/C1 = 1.0	0% C1	2943 ± 7	2.61	Ti/C2 = 1.0	0% TiC	2777 ± 6	0.75
	2% C1	2769 ± 6	1.84		1% TiC	2763 ± 6	0.72
	5% C1	2730 ± 6	1.51		3% TiC	2644 ± 6	0.60
	8% C1	2647 ± 6	1.28		4% TiC	2635 ± 6	0.59
	12% C1	2466 ± 6	1.14		6% TiC	2563 ± 6	0.45
	17% C1	2268 ± 5	0.97		9% TiC	2511 ± 6	0.42
					12% TiC	2424 ± 6	0.38
					15% TiC	2364 ± 5	0.33
Ti/C1 = 1.3	0% TiC	2836 ± 6	2.24				
	5% TiC	2755 ± 6	1.71				
	10% TiC	2694 ± 6	1.41				
	15% TiC	2642 ± 6	1.24				
	17% TiC	2584 ± 6	0.98				
	20% TiC	2526 ± 6	0.73				
	25% TiC	2459 ± 5	0.63				

bustion wave velocities were obtained by measuring the passage of the combustion wave between the two thermocouple tips located near the middle of the sample.

To study the infiltration characteristics of liquid titanium through capillaries of graphite and furnace black, we observed the morphology and compositions of reaction products, which were synthesized from the uncompacted reactant mixtures. The amount of unreacted titanium and carbon in the titanium carbide products was analysed by a wet chemical method.

Reaction couples of a titanium disc and a furnace black disc, and a titanium disc and a graphite block were prepared to study the reaction interface. A titanium disc (20 mm in diameter and 3 mm in thickness) was prepared at uniaxial compaction of 90 MPa. To prepare the furnace black disc, 10 g of furnace black powder (C3) were placed in a graphite die (50 mm in diameter), hot-pressed at 20 MPa under nitrogen atmosphere and held at 1500 °C for 20 min, with heating and cooling rates of 50 °C min^{-1}. A polished graphite block (30 × 30 × 10 mm) was also prepared for the reaction couple. The reaction couple experiment was performed under argon atmosphere in a graphite furnace. The reaction couple was heated up to 1662 °C or 1690 °C with a heating rate of 20 °C min^{-1}, and without holding, cooled down to the room temperature with a cooling rate of 20 °C min^{-1}. The polished cross-sections and reacted surfaces of reaction couples were examined using OM, SEM, WDS, and XRD with CuK_α radiation.

3. Results and discussion

The combustion parameters with graphite as a carbon source are shown in Table II. Fig. 2 shows the combustion temperature and wave velocity as a function of the amount of TiC diluent mixed with a stoichiometric reactant mixture (Ti/C = 1.0). Powders of C1 graphite, C2 graphite, amorphous furnace black of Vulcan XC-72 (C3), and Black Pearls 120 (C4) were used as carbon sources. An adiabatic temperature is thermodynamically calculated by assuming

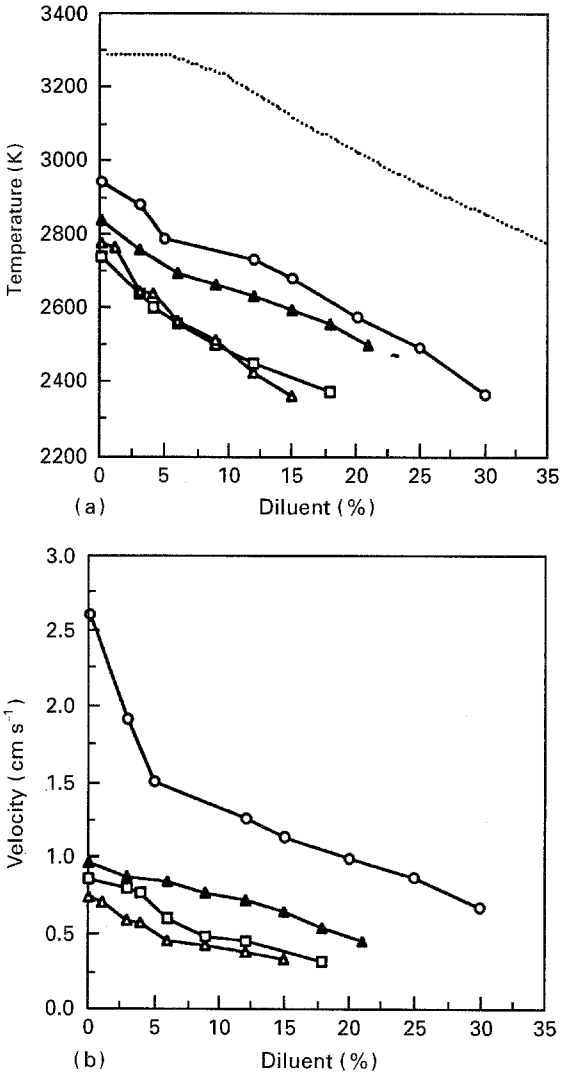

Figure 2 (a) Combustion temperature and (b) combustion wave velocity as a function of the amount of TiC diluent for various carbon sources. Ti and C ratio was fixed at 1.0. ----- T_{ad}; ○ Ti/C1; △ Ti/C2; ▲ Ti/C3; □ Ti/C4.

that all of the heat released by the reaction ultimately is used to raise the temperature of the sample without any heat losses. The real combustion temperature is usually lower than the adiabatic temperature, mainly

due to heat losses during the reaction. The combustion temperatures of compacts with different carbon sources is shown in Fig. 2(a). The combustion temperature is lowered by adding TiC powder as a diluent and TiC powder only acts as a heat sink without participating in the reaction. In the TiC combustion synthesis with various carbon sources, the combustion temperature was higher in the order of C1 graphite, C3 furnace black, C2 graphite, and C4 furnace black. As shown in Fig. 2(b), the combustion wave velocity of the compact with a molar ratio of Ti/C = 1.0 without any TiC diluent was 2.61 cm s^{-1} for C1, 0.98 cm s^{-1} for C3, 0.87 cm s^{-1} for C4, and 0.75 cm s^{-1} for C2, respectively. The combustion wave velocity decreased as TiC diluent was added in the similar way as the combustion temperature. This is because the combustion wave velocity strongly depends on the combustion temperature. Fig. 2 suggests that the apparent reactivity of titanium powder with C1 graphite powder is higher than with the C2 graphite and furnace black (C3 and C4) powder. When 30 wt % TiC powder was added as a diluent to the sample with molar ratio of Ti/C1(graphite) = 1.0, the combustion wave velocity fell down to 0.69 cm s^{-1}, approximately one-quarter of the wave velocity of the sample without any diluent. When TiC powder above 21 wt % was added to the sample with the C2 graphite and furnace black (C3, C4) carbon sources, propagation did not occur. The C1(graphite, 5 μm) powder shows a higher reactivity than C2 (graphite, 15.2 μm) because the increase in the particle size results in the decrease of the contact area between reactants.

Fig. 3 shows Arrhenius plots of $\ln[(1-w)^{1/2}u/T_c]$ versus $1/T_c$, which were calculated from the combustion temperature and wave velocity data. Combustion temperature and wave velocity were varied by adding various amounts of TiC to the sample with molar ratio of Ti/C1 (graphite) = 1.0 (Fig. 3(a)), by adding excess C1 (graphite) to the sample with molar ratio of Ti/C1 (graphite) = 1.0 (Fig. 3(b)), and by adding TiC to the sample with molar ratio of Ti/C1 (graphite) = 1.3 (Fig. 3(c)).

The activation energies for the high temperature region in Fig. 3(a), (b) and (c) were 399 ± 36, 294 ± 33, and 400 ± 13 kJ mol^{-1}, respectively. It was reported that the activation energy for carbon diffusion through solid TiC is approximately in the range of 234–410 kJ mol^{-1}, depending on the method of measurement [33–37]. A low activation energy (below about 300 kJ mol^{-1}) was observed in the measurement from reaction couple between liquid Ti and C [36] while the activation energy higher than about 300 kJ mol^{-1} was observed in the measurement either from diffusion couple between TiC (single crystal) and C [35] or TiC (single crystal) and Ti [37]. The large variation of activation energy is reported to be due to the concentration of defects, which gives high-rate diffusion path in TiC and strongly affects the diffusivity of carbon through TiC [37]. It is believed that the activation energy will be smaller when the defects of fast diffusion-path source are more abundant in the reaction product layer. On the other hand, it is reported that the activation energy for the diffusion of Ti through TiC is 738 kJ mol^{-1} and that the diffusion rate of Ti through TiC is approximately four orders of magnitude slower than that of C through TiC [38]. Therefore, the activation energies for the high temperature region in Fig. 3 suggest that the combustion reaction rate for TiC is controlled by the diffusion of carbon through TiC.

In the lower temperature region in Fig. 3(a) and (b) the rate of decrease in the combustion velocity becomes smaller as the amount of diluent is increased.

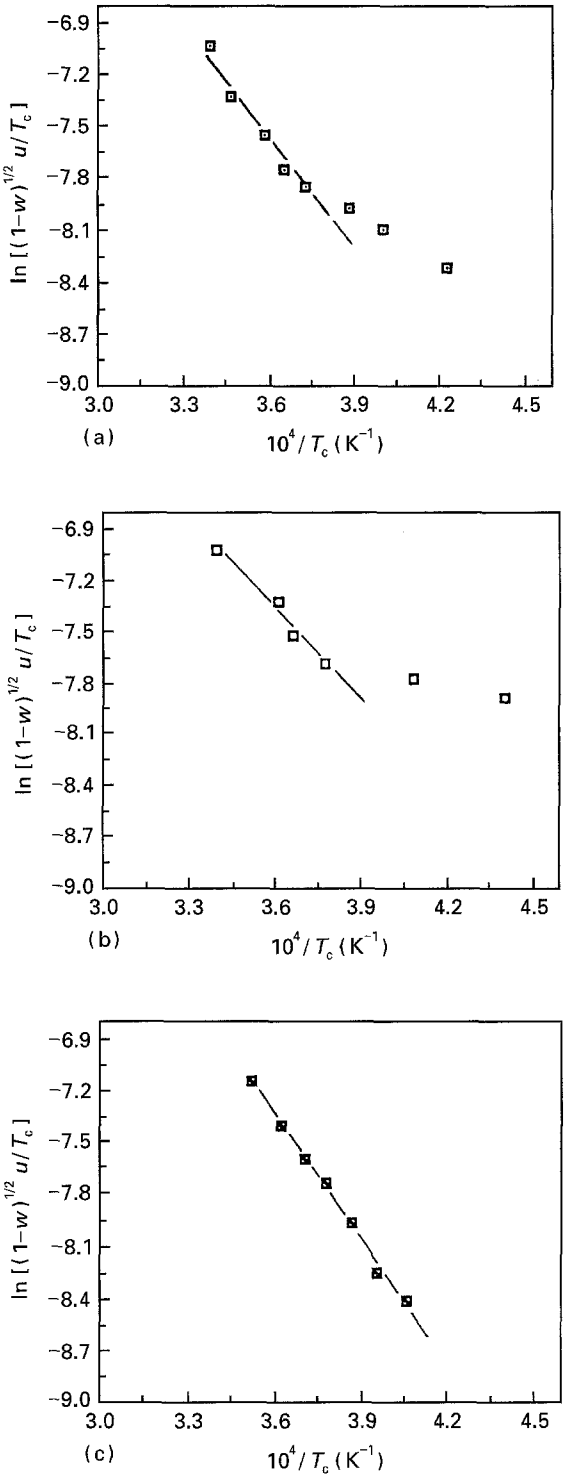

Figure 3 Arrhenius plot of $\ln[(1-w)^{1/2}u/T_c]$ versus $1/T_c$ in TiC combustion synthesis using graphite carbon source (C1, 5 μm). (a) Ti/Cl (graphite) = 1.0, TiC diluent, $E = 399 \pm 36$ kJ mol^{-1}, (b) Ti/C1 (graphite) = 1.0, C1 excess, $E = 294 \pm 33$ kJ mol^{-1}; (c) Ti/C1 (graphite) = 1.3, TiC diluent, $E = 400 \pm 13$ kJ mol^{-1}.

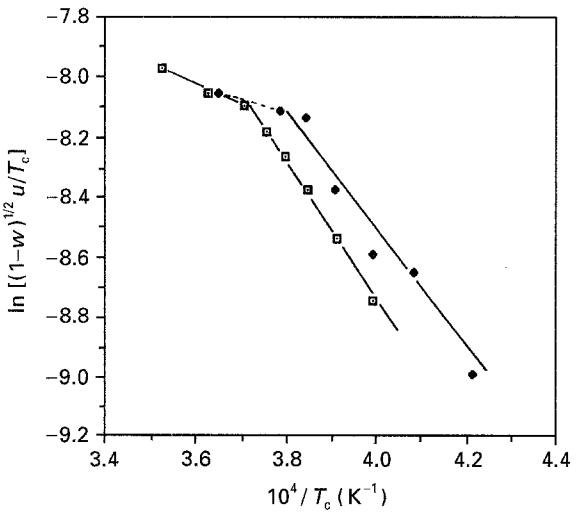

Figure 4 Arrhenius plot of $\ln[(1-w)^{1/2}u/T_c]$ versus $1/T_c$ in TiC combustion synthesis using furnace black carbon sources of Vulcan XC-72 (C3, 0.030 μm ⊡, $E = 380 \pm 13\,kJ\,mol^{-1}$) and Black Pearls 120 (C4, 0.075 μm ◆, $E = 350 \pm 29\,kJ\,mol^{-1}$). In the high temperature region, $E = 108 \pm 15\,kJ$.

The reason is not clear at this moment but we believe that the change in the thickness of diffusion barrier and the generation of defects from thermal stress lowers the resistance against the reactant migration. During the combustion reaction, liquid titanium infiltrates into the boundaries between particles and wets the particles. By adding a diluent, the combustion temperature is decreased and the thickness of liquid Ti layer which surrounds graphite particles is also decreased because Ti concentration in the reactant mixture decreases. During the combustion reaction between Ti and C, it is expected that many defects and fissures are formed in the product layer of TiC by mechanical and thermal stresses from the reaction interface. The mechanical stress is mainly due to the volume change. For the combustion reaction of Ti and C to form TiC, the decrease of intrinsic volume is calculated to be approximately 24% [39]. As the thickness of TiC product layer formed from the reaction interface is thinner, a resistance to the diffusion of carbon through product layer is lowered [40].

Fig. 4 shows the Arrhenius plot of $\ln[(1-w)^{1/2} \times u/T_c]$ versus $1/T_c$ from the measurements of combustion temperature and wave velocity, varied by adding various amounts of TiC diluent to the sample with molar ratio of Ti/C3 (furnace black) = 1.0 and Ti/C4 (furnace black) = 1.0. The change in slope was observed at approximately 2638 and 2696 K, respectively. When Vulcan XC-72 (C3) was used as a carbon source, the activation energy for the high temperature region was $108 \pm 15\,kJ\,mol^{-1}$. It was reported that the activation energy for the dissolution of carbon into liquid titanium is in the range of 78 to 117 $kJ\,mol^{-1}$ [28, 36]. A dissolution–precipitation mechanism, where a carbon dissolves into liquid titanium and TiC is subsequently precipitated from the liquid titanium, might play a role in the high temperature region. The activation energies of 350 ± 29 and $380 \pm 13\,kJ\,mol^{-1}$ for the low temperature region suggest that the reaction is controlled by a carbon diffusion through TiC product layer. The result agrees well with that of Dunmead and co-workers [28] using furnace black of Monarch 905 as a carbon source. We believe that carbon dissolution mechanism is not observed in the graphite–Ti system due to the large particle size of graphite used in the experiment. Also the reactivity of graphite is higher than amorphous carbon which might be due to the structural difference between graphite and amorphous carbon.

The wetting angle of liquid iron and carbon is reported to be apporximately 37° [41]. The surface energy of liquid iron is similar to that of liquid titanium at approximately 1650 dyne/cm [42], and thus it is guessed that the wetting angle between liquid titanium and solid carbon is also approximately 37°. In a wetting system, infiltration flow velocity through a capillary is linearly proportional to the capillary radius [43] which increases with the size of the powder. In this work, the graphite powder is much larger than furnace black and so liquid titanium will infiltrate much faster through the capillary of graphite powders. In addition to the effect of the carbon particle size on the titanium infiltration, the agglomeration of the fine furnace black powders will also prevent the penetration of the liquid titanium into pores between particles.

To confirm the infiltration characteristics of liquid titanium through the pores of carbon powders, the combustion reaction was performed by igniting reactant mixtures of Ti/C1 (graphite) = 1.0 and Ti/C3 (furnace black) = 1.0 which were charged into the glass bottles without any compaction in order to remove the effect of compact density.

Fig. 5 shows the scanning electron micrographs of the products combustion synthesized from uncompacted mixture of (a) Ti/C1 (graphite) = 1.0 and (b) Ti/C3 (furnace black) = 1.0. While a considerable amount of unreacted carbon was observed in the sample combustion synthesized with furnace black, it was not observed with the graphite carbon source. This indicates that the infiltration characteristics of liquid titanium through graphite powder is much better than through furnace black powder. Fig. 6 shows the XRD pattern of samples shown in Fig. 5. The crystallinity of TiC_{1-x} in Fig. 6(a) was better than that in Fig. 6(b). Furthermore, unreacted titanium phase was found in (b) while it was not in (a). The lattice parameter of titanium carbide in Fig. 6(a) and (b) were 0.4328 and 0.4294 nm which approximately corresponds to that of $TiC_{0.95}$ and $TiC_{0.5}$, respectively [16]. The fact that TiC_{1-x} with high substoichiometry is more likely to be formed in the reaction of Ti and furnace black is because the infiltration velocity of liquid titanium through the pores of furnace black powder is much lower than graphite.

Fig. 7 shows the amount of unreacted titanium in the products which were synthesized from molar ratio of Ti/C1 (graphite) and Ti/C3 (furnace black) between 1.0 and 1.6. As the molar ratio of Ti/C was increased, the amount of unreacted titanium was gradually increased from 0.066 wt% to 0.485 wt% with graphite while it was increased from 0.308 wt% to 0.753 wt% with furnace black.

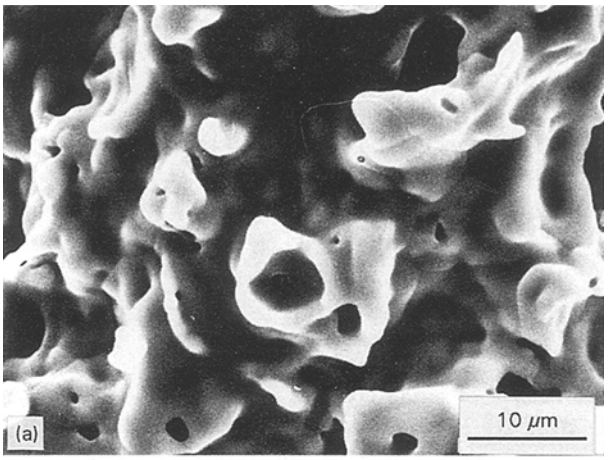

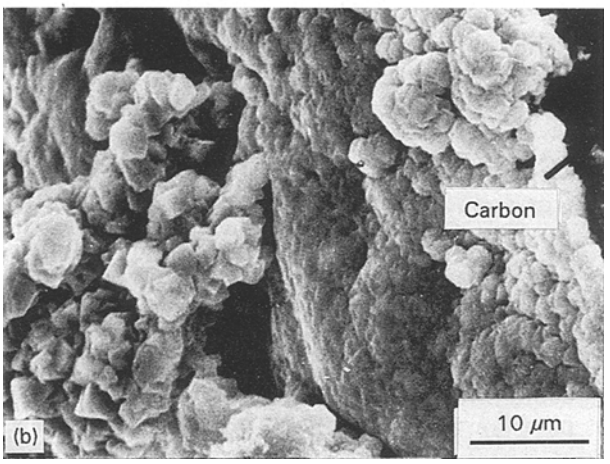

Figure 5 Scanning electron micrographs of the samples combustion synthesized from uncompacted reactant mixtures with molar ratio of (a) Ti/C1 (graphite) = 1.0 and (b) Ti/C3 (furnace black) = 1.0.

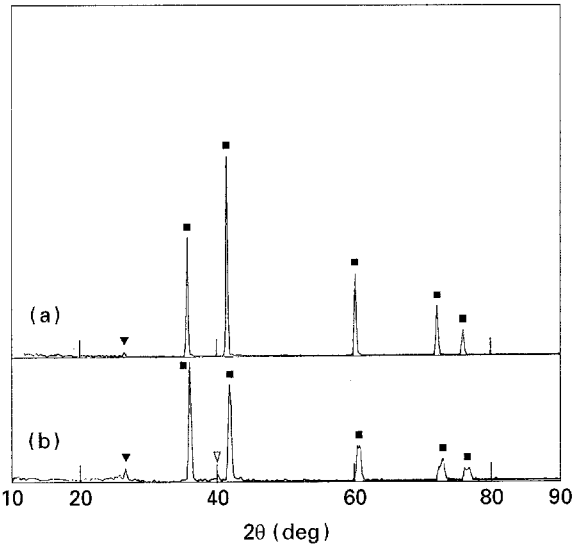

Figure 6 X-ray diffraction patterns of the product combustion synthesized from uncompacted reactant mixtures with molar ratio of (a) Ti/C1 (graphite) = 1.0 and (b) Ti/C3 (furnace black) = 1.0. ■ TiC; ▼ C; ▽ Ti.

Fig. 8(a) shows the polished cross-section of reaction couple of a titanium disc and a furnace black disc prepared at 1690 °C. A TiC layer was formed at the carbon and Ti interface and particles were precipitated in the Ti matrix. Fig. 8(b) shows the concentration distribution of Ti and C in a precipitated particle, which proved that the particle was titanium carbide precipitated in Ti melt. The results of Fig. 8 suggest that the TiC layer between titanium and carbon was formed by the carbon diffusion through TiC while TiC particles in titanium matrix were formed by the carbon dissolution and TiC precipitation. It should be noted that the dissolution of carbon into liquid titanium will occur via dissolution of highly substoichiometric TiC_{1-x} with a low melting temperature, which is formed by the reaction of titanium-rich

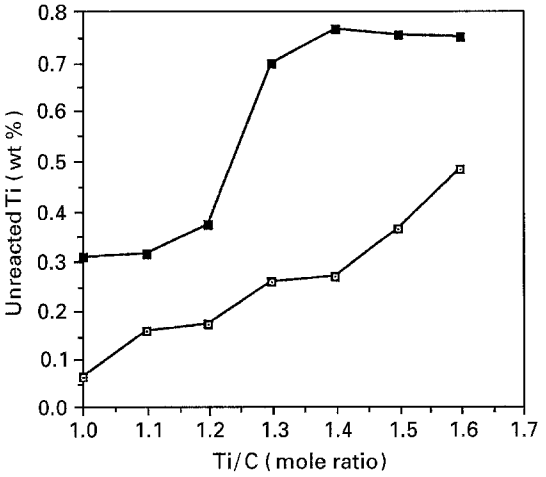

Figure 7 Weight percent of unreacted titanium in combustion synthesized titanium carbide as a function of molar ratio of (□) Ti/C1 (graphite) or (■) Ti/C3 (furnace black).

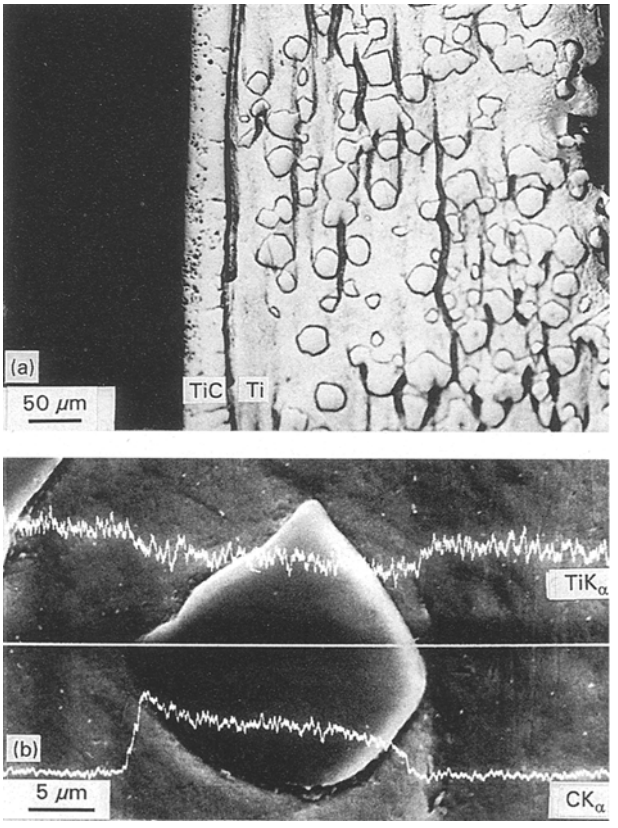

Figure 8 (a) Optical micrograph of the polished cross-section of the reaction couple and (b) concentration profile of Ti and C in a precipitated particle. The reaction couple (titanium disc–furnace black disc) was formed at 1690 °C.

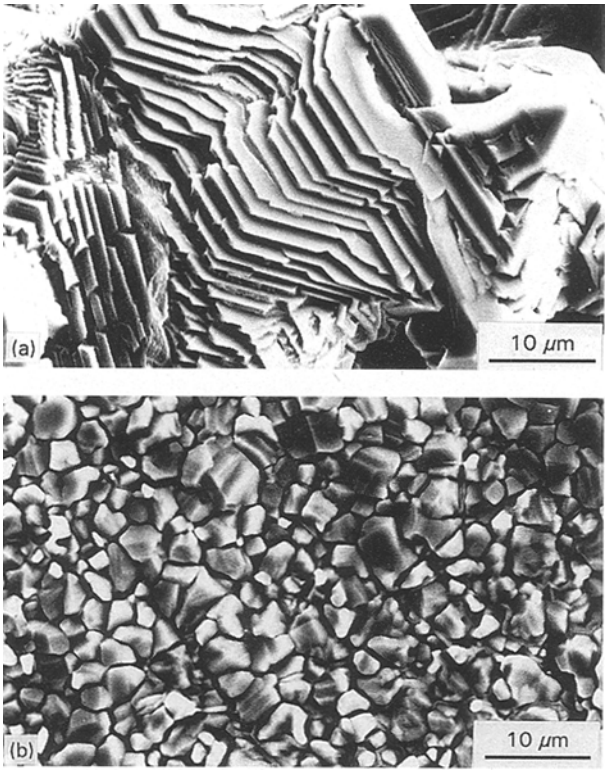

Figure 9 Scanning electron micrographs of reaction couple (titanium disc–graphite block) formed at 1662 °C. (a) TiC on titanium pellet and (b) TiC on graphite block.

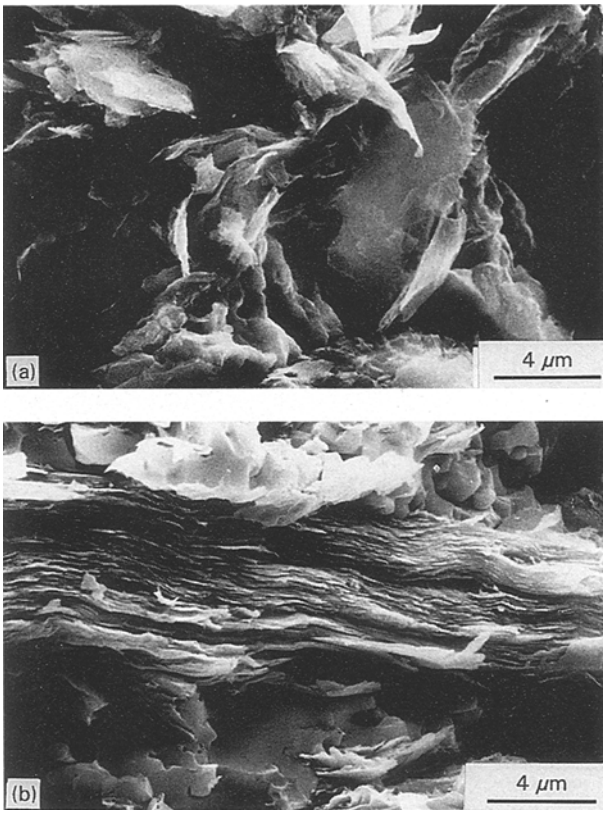

Figure 10 Scanning electron micrographs of the fractured surface from combustion synthesized TiC pellet. (a) Ti/C1 (graphite) = 0.5 and (b) Ti/C2 (graphite) = 1.0 mixed with 15 wt% TiC.

reactant mixture. This is because the reaction between titanium and carbon is so fast that the direct dissolution of carbon into liquid titanium without TiC_{1-x} formation would be impossible [41]. Therefore, it is believed that TiC formation by the carbon dissolution and TiC precipitation mechanism occurs after highly substoichiometric TiC_{1-x} is formed at the interface as shown in Fig. 8(a). As mentioned already in Fig. 6, the substoichiometric TiC_{1-x} is more likely to be formed in the case of furnace black carbon source. The results of Figs 6 and 7 support the fact that the carbon dissolution and TiC precipitation mechanism discussed in Fig. 4 can occur with the furnace black carbon source.

Fig. 9 shows the reacted surface in the reaction couple of titanium disc and graphite block formed at 1662 °C, below the melting point of titanium. After the reaction, most of the TiC formed was adhered to the Ti disc and separated from the graphite block because of the weak bond between the layers of graphite. The morphology of reaction products formed on the Ti disc and graphite block are shown in Fig. 9(a) and (b), respectively. Fig. 9(a) shows a layered structure on the Ti disc, which was proved to be titanium carbide by XRD. This suggests that graphite fissured in thin layers during the reaction and liquid titanium infiltrated into the layer to wet the surface of graphite. The morphology of the graphite side with island structure is shown in Fig. 9(b), which was also proved to be titanium carbide by XRD. Its cross-section showed that it was a dense TiC film of approximately 3 μm in thickness. The film was believed to be formed by the reaction between titanium vapour and solid carbon surface and the Ti (vapour)–C (solid) might partly participate in the combustion reaction between titanium and carbon.

The morphology as a fissured form in thin layers was also observed in the TiC combustion synthesis from reaction mixtures with composition of Ti/C1 (graphite) = 0.5 and Ti/C2 (graphite) = 1.0 mixed with 15 wt% TiC. This is shown in Fig. 10. This is attributed to the structural characteristics of graphite, with weak van der Waals bonds between the layers and anisotropic thermal expansion [45] (in the direction perpendicular to the basal plane, it is about one-third higher than that in the parallel direction), and the mechanical and thermal stresses from the reaction interface between Ti and C.

4. Conclusions

From the combustion temperature and combustion wave velocity measurements, it was observed that the apparent reactivity of titanium with graphite powder was higher than with amorphous carbon black powder. During the combustion reaction between graphite and titanium, the graphite fissured layer by layer in the parallel direction with the basal plane because of its crystal structure. Thus, the reaction between graphite and liquid titanium was accomplished mainly on the surface of the thinly fissured layer.

When the graphite powder was used as a carbon source in TiC combustion synthesis, the carbon diffusion through TiC is the rate-controlling process. It was also believed that the carbon diffusion through

TiC was affected by the thickness of reaction product layer and also defects formed by the thermal stress during the reaction. Titanium carbide synthesized with graphite contains less unreacted carbon and is more close to the stoichiometric TiC.

Acknowledgements

This research was supported by Research Institute of Industrial Science and Technology, and Engineering Research Center for Interface Science and Technology of Materials.

References

1. J. B. HOLT and Z. A. MUNIR, *J. Mater. Sci.*, **21** (1986) 251.
2. K. S. VECCHIO, J. C. LASALVIA, M. A. MEYERS and G. T. GRAY III, *Metall. Trans. A* **23A** (1992) 87.
3. J. B. HOLT, D. D. KINGMAN and G. M. BIANCHINI, *Mater. Sci. Eng.* **71** (1985) 321.
4. T. KOTTKE, L. J. KECSKES and A. NIILER, *AIChE J.* **36** (1990) 1581.
5. M. E. GRAMI and Z. A. MUNIR, *J. Amer. Ceram. Soc.* **73** (1990) 1235.
6. Y. MIYAMOTO, *Ceram. Bull.* **69** (1990) 686.
7. S. D. DUNMEAD, Z. A. MUNIR, J. B. HOLT and D. D. KINGMAN, *J. Mater. Sci.* **26** (1991) 2410.
8. V. I. ITIN, A. D. BRATCHIKOV, A. G. MERZHANOV and V. M. MASLOV, *Combust. Explos. Shock Waves* (Engl. Transl.) **17** (1981) 293.
9. K. A. GABRIEL, S. G. WAX and J. W. McCLAULEY, in Proceedings of the DARPA/Army Symposium on Self-Propagating High-Temperature Synthesis, Daytona Beach, (Watertown, MA, 1985) p. 105.
10. S. ADACHI, T. WADA, T. MIHARA, Y. MIYAMOTO and M. KOIZUMI, *J. Amer. Ceram. Soc.* **73** (1990) 1451.
11. B. H. RABIN, G. E. KORTH and R. L. WILLIAMSON, *ibid.* **73** (1990) 2156.
12. O. ODAWARA, *ibid.* **73** (1990) 629.
13. A. G. MERZHANOV and B. I. KHAIKIN, *Prog. Energy Combust. Sci.* **14** (1988) 1.
14. A. A. ZENIN, *Pure Appl. Chem.* **62** (1990) 889.
15. W. L. FRANKHOUSER, K. W. BRENDLEY, M. C. KIESZEK and S. T. SULLIVAN, "Gasless combustion synthesis of refractory compounds" (Noyes Publications, Park Ridge, New Jersey, USA, 1985) p. 5.
16. E. K. STORMS, "The refractory carbides" (Academic Press, New York, 1967) p. 1.
17. R. J. KERANS, K. S. MAZDIYASNI, R. RUH and H. A. LIPSITT, *J. Amer. Ceram. Soc.* **67** (1984) 34.
18. S. G. VADCHENKO, Y. M. GRIGOR'EV and A. G. MERZHANOV, *Combust. Explos. Shock Waves* (Engl. Transl.) **12** (1976) 606.
19. M. A. KORCHAGIN and V. V. ALEKSANDROV, *ibid.* **17** (1981) 58.
20. K. A. GABRIEL, S. G. WAX, and J. W. McCLAULEY, in Proceedings of the DARPA/Army Symposium on Self-Propagating High-Temperature Synthesis, Daytona Beach, (Watertown, MA, 1985) p. 403.
21. A. S. ROGACHEV, A. S. MUKASY'AN and A. G. MERZHANOV, *Dokl. Phys. Chem.* **297** (1987) 1240.
22. J. WONG, E. M. LARSON, J. B. HOLT, P. A. WAIDE, B. RUPP and R. FRAHM, *Science* **249** (1990) 1406.
23. Y. CHOI and S. RHEE, *J. Mater. Sci.* **28** (1993) 6669.
24. *Idem., J. Mater. Res.* **8** (1993) 3202.
25. *Idem., J. Mater. Sci. Lett.* **13** (1994) 323.
26. I. BARIN, F. SAUERT, E. SCHULTZE-RHONHOF and W. S. SHENG, "Thermochemical data of pure substances" (VCH, New York, 1989) p. 1528.
27. B. I. KHAIKIN and A. G. MERZHANOV, *Combust. Explos. Shock Waves* (Engl. Transl.) **2** (1966) 22.
28. S. D. DUNMEAD, Z. A. MUNIR and J. B. HOLT, *J. Amer. Ceram. Soc.* **75** (1992) 175.
29. *Idem., ibid.* **75** (1992) 180.
30. K. KINOSHITA, "Carbon" (John Wiley and Sons, New York, 1988) p. 23.
31. A. I. KIRDYASHKIN, YU. M. MAKSIMOV and E. A. NEKRASOV, *Combust. Explos. Shock Waves* (Engl. Transl.) **17** (1981) 377.
32. S. D. DUNMEAD, D. W. READEY, C. E. SEMLER and J. B. HOLT, *J. Amer. Ceram. Soc.* **72** (1989) 2318.
33. S. SARIN, *J. Appl. Phys.* **39** (1968) 3305.
34. *Idem., ibid.* **39** (1968) 5036.
35. D. L. KOHLSTEDT, W. S. WILLIAMS and J. B. WOODHOUSE, *ibid.* **41** (1970) 4476.
36. L. ADELSBERG and L. CADOFF, *Trans. AIME.* **24** (1967) 933.
37. C. J. QUINN and D. L. KOHLSTEDT, *J. Amer. Ceram. Soc.* **67** (1984) 305.
38. S. SARIN, *J. Appl. Phys.* **40** (1969) 3515.
39. R. W. RICE and W. J. McDONOUGH, *J. Amer. Ceram. Soc.* **68** (1985) c122.
40. H. SCHMALZRIED, "Solid State Reactions", 2nd edn (Verlag Chemie, Weinheim, Deerfield Beach, FL 1981) p. 116.
41. L. C. DUFOUR, C. MONTY and G. P. ERVAS, "Surfaces and interfaces of ceramic materials" (Kluwer Academic Publishers, Dordrecht, Boston, and London, 1988) p. 173.
42. C. T. LYNCH, "CRC Handbook of materials science, Vol. I, General Properties" (CRC Press, Inc., Boca Raton, Florida, 1974) p. 109.
43. J. S. REED, "Introduction to the principles of ceramic processing" (John Wiley and Sons, New York, 1989) p. 24.
44. A. OYA and S. OTANI, *Carbon* **17** (1979) 131.
45. K. KINOSHITA, "Carbon" (John Wiley and Sons, New York, 1988) p. 13.

Received 18 May 1994
and accepted 22 March 1995